NASA TN D-1384

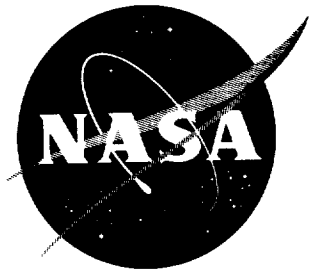

TECHNICAL NOTE

D-1384

A WIND-TUNNEL INVESTIGATION AT A MACH NUMBER OF 2.01 OF THE SONIC-BOOM CHARACTERISTICS OF THREE WING-BODY COMBINATIONS DIFFERING IN WING LONGITUDINAL LOCATION

By Odell A. Morris

Langley Research Center
Langley Station, Hampton, Va.

NATIONAL AERONAUTICS AND SPACE ADMINISTRATION

WASHINGTON September 1962

NATIONAL AERONAUTICS AND SPACE ADMINISTRATION

TECHNICAL NOTE D-1384

A WIND-TUNNEL INVESTIGATION AT A MACH NUMBER OF 2.01 OF THE SONIC-BOOM CHARACTERISTICS OF THREE WING-BODY COMBINATIONS DIFFERING IN WING LONGITUDINAL LOCATION

By Odell A. Morris

SUMMARY

A wind-tunnel investigation has been conducted at a Mach number of 2.01 to determine the sonic-boom characteristics of three wing-body configurations having different longitudinal locations of the wing. Wind-tunnel measurements of the pressure fields generated by the models (fuselage length of 1 inch) were made for three different horizontal positions at stations up to 50 body lengths from the models and for lift coefficients up to 0.2. Comparison of the measured adjusted wind-tunnel sonic-boom pressures with theoretical values showed reasonable agreement and, in general, most of the computed values were within a range of ±15 percent of the adjusted measured bow-shock pressures. These results should prove to be useful along with previously obtained data in making generalized studies of the effects of configuration variables on the sonic-boom characteristics.

INTRODUCTION

The importance of the sonic boom is now well recognized and to date a considerable number of studies have been made on the subject. (For example, see refs. 1 to 4.) In an effort to supply more information concerning the influence of configuration design on the effect of sonic boom, several investigations have been undertaken in the Langley 4- by 4-foot supersonic pressure tunnel. The tests reported in reference 5 provide some data on the effects of model thickness distribution on the sonic-boom intensity, and the investigation of reference 6 has presented information on the effects of lift on the sonic-boom intensity for several wing-body configurations with variations in wing area. As a continuation of this program, the present investigation was undertaken to supply additional experimental information on the sonic-boom characteristics of three wing-body configurations for correlation with theoretical results.

The tests were performed at a Mach number of 2.01 on three wing-body configurations with variation in the longitudinal position of the wing. Pressures in the model flow fields were measured at three different separation distances and for several angles of attack. The experimental results are compared with theory.

SYMBOLS

C_L	lift coefficient
$\bar{c}$	mean aerodynamic chord of wing
A	cross-sectional area (normal to free stream) of wing-body combination, sq in. (fig. 3)
L	length of models, in.
M	Mach number
p	free-stream static pressure, reference pressure
p_l	local static pressure measured at the probe surface
Δp	pressure difference, $p_l - p$
Δp_{max}	maximum value of Δp at the bow shock
$\left(\frac{\Delta p}{p}\right)_{max}$	maximum pressure ratio at bow shock
x,r	cylindrical coordinates of bodies of revolution (fig. 2)
X,Y	Cartesian coordinates of field point, X measured in free-stream direction from model nose, in. (fig. 4)
ΔX	distance from bow shock to point of zero pressure
δX	change in position of bow shock due to vibration

Models and Tests

A photograph of the three models investigated is shown in figure 1. Figure 2 shows a drawing of these model configurations and gives the principal dimensions of the models and the body coordinates. The

60° delta wing planform used on each model had a thickness of 4.8 percent chord with circular-arc wing sections. The cross-sectional-area distributions (normal to free stream) of the actual wing-body models are shown in figure 3. This M = 1.0 distribution was assumed to be adequate for theoretical considerations contained herein on the basis of the study presented in reference 6. As may be noted, both the maximum cross-sectional area and its longitudinal distribution were considerably different for the three configurations.

The investigation was conducted in the Langley 4- by 4-foot supersonic pressure tunnel at a Mach number of 2.01 and a Reynolds number per foot of 2.5×10^6. A sketch of the test apparatus is shown in figure 4. The models were sting mounted on a remotely controlled support system which provided longitudinal motion of the models. Measurements of the pressure field were made by three probes located at vertical distances of 12.5, 25, and 50 inches below the model, which was in an inverted position for the tests. A fourth probe, also mounted at the 50-inch station just forward of the model pressure field was used to measure the tunnel reference pressure. Four probe orifices 0.013 inch in diameter were spaced 90° apart around each probe and were arranged to lie within a Mach cone originating at the model apex. Each change in angle of attack was made manually before each test by bending the model sting. The angles of attack, which were set for desired lift coefficients of 0, 0.1, and 0.2 were based on a lift-curve slope of 0.037 for the wing-body combinations.

RESULTS AND DISCUSSION

The data of figure 5 present the measurements of the pressure fields of each of the three models at lift coefficients of 0, 0.1, and 0.2. Pressures and distances are plotted in parametric form in accordance with theoretical considerations which facilitates comparison of the shapes of the pressure fields for various separation distances. The parameters plotted are $\frac{\Delta p}{p}\left(\frac{Y}{L}\right)^{3/4}$ as a function of $\frac{\Delta x}{L}\Big/\left(\frac{Y}{L}\right)^{1/4}$. According to the theory of reference 7, pressure fields for a given model and lifting condition, when plotted in this form, will be identical with a characteristic N-shape at any distance if far-field conditions exist. From an inspection of the data, models A and B appear to have reached far-field conditions at the extreme station of Y/L of 50. However, for the wing-body combination with the rearward wing position (model C), far-field conditions do not appear to be fully obtained at a lift coefficient of 0.1. Figure 5(c) indicates that for model C $\left(\text{when } C_L = 0.1\right)$, the characteristic N-shaped sonic-boom pressure curve has not completely developed, although the maximum bow-shock pressures appear to have nearly reached far-field values.

The data of figure 6 show a comparison of the tunnel measurements of the pressure rise at the bow shock with theoretical values for the three configurations investigated. The theoretical values of the bow-shock pressures were computed in the same manner as described in reference 7, which was based on a derivation of Walkdens equation (ref. 1). Tunnel data are presented both as measured and with adjustments. The adjustments of the wind-tunnel measurements of the bow-shock strength were made to compensate for model vibration according to the method derived in reference 7. For convenience, Carlson's method for obtaining the adjusted values as given in reference 7 is repeated herein in the appendix. Comparison of the theory with the adjusted values shows reasonable agreement. Some discrepancies, however, were shown for all three wing positions. The adjusted tunnel data for models A and B show a marked increase in bow-shock strength, with increasing lift coefficient throughout the lift-coefficient range. The adjusted data for these models are in general agreement with the theory except that the measured rate of increase is somewhat less for model A. In contrast to the data for models A and B, that for model C show only a small increase in shock strength with increasing lift coefficient up to $C_L = 0.1$ with a rapid rise beyond that point. This behavior is also in general agreement with the theory.

The summary plot of figure 7 shows that most of the theoretically computed points fall within a range of ±15 percent of the adjusted bow-shock pressures. It is believed that part of the discrepancies between the theoretical and experimental data may be due to flow-separation effects on the models in the region of the trailing edge of the wing-body juncture, where some fairly sharp slope changes exist in the body shape. (See fig. 2.) Also as was pointed out in reference 7, possible interference effects which are not covered by the theory may occur between the model components. Despite the discrepancies, these results should prove to be useful along with previously obtained data in making generalized studies of the effects of configuration variables on the sonic-boom characteristics.

CONCLUDING REMARKS

An investigation has been conducted in the Langley 4- by 4-foot supersonic pressure tunnel at a Mach number of 2.01 to measure the sonic-boom characteristics of three wing-body configurations and to correlate the experimental results with theory. Comparison of adjusted wind-tunnel values with theoretical values showed reasonable agreement and, in general, most of the computed values were within a range of ±15 percent of

the adjusted measured bow-shock pressures. These results should prove to be useful along with previously obtained data in making generalized studies of the effects of configuration variables on the sonic-boom characteristics.

Langley Research Center,
National Aeronautics and Space Administration,
Langley Station, Hampton, Va., June 4, 1962.

APPENDIX

ADJUSTMENTS OF WIND-TUNNEL MEASUREMENTS OF BOW-SHOCK STRENGTH TO COMPENSATE FOR MODEL VIBRATION (FROM REF. 7)

The following method for adjusting the measurements of bow-shock strength to compensate for model vibration is taken from reference 7. Consider a completely steady model in uniform supersonic flow and an ideal pressure sensing system with a probe at a distance large enough so that a true far-field N-wave is recorded, as represented by the heavy dashed line in the following sketch:

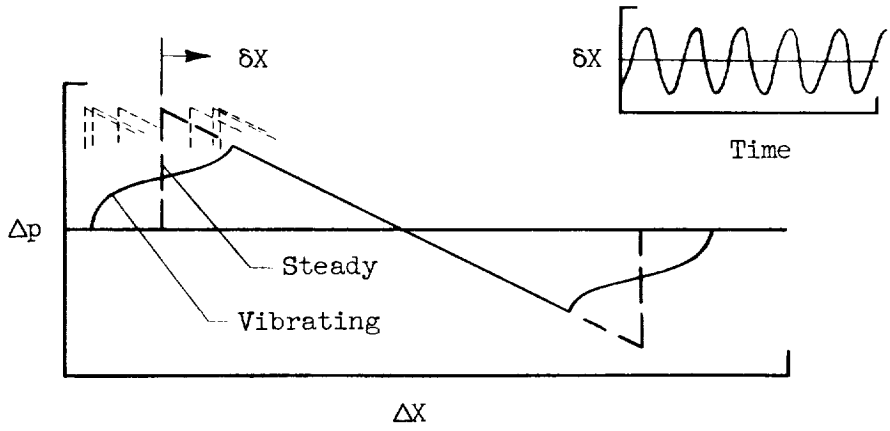

Now suppose that the model undergoes a constant amplitude vibratory motion represented by the inset sketch. In this case the N-wave will occupy successive positions at equal time increments as indicated by the light dashed lines on the pressure plot. At a given probe location a highly damped measuring system such as the one used for these tests would register a time average of the pressures imposed on it. When a range of probe locations is considered, the measured pressures with a constant-amplitude vibrating system take on the appearance of the solid-line curve. This curve does not resemble the actual wind-tunnel data, but it is not likely that tunnel vibration is confined to the single amplitude shown here.

When a varying amplitude is considered, the resulting pressure curve assumes the characteristics of that shown in the next sketch:

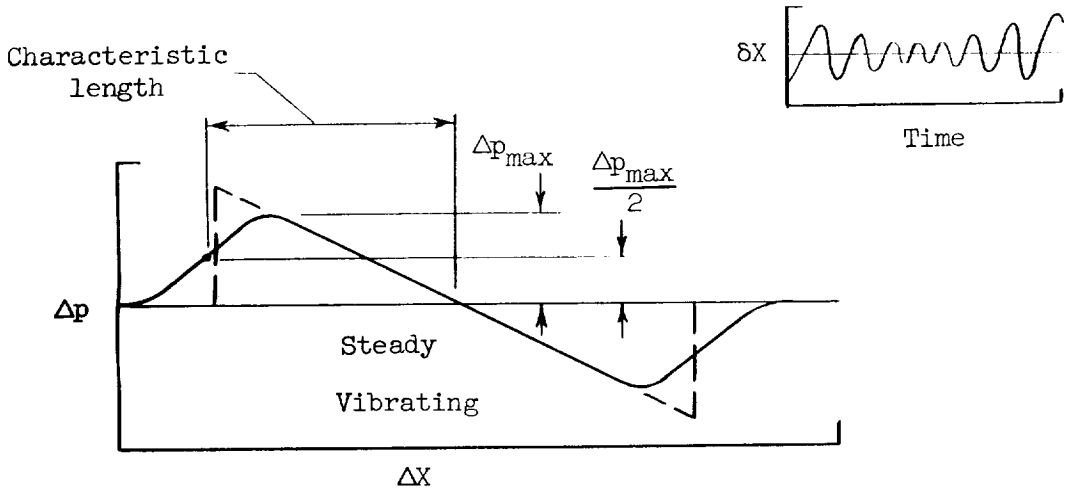

The assumed amplitude-time relationship is shown in the inset. The curve now resembles those obtained from actual tunnel measurements.

In both of the above sketches, note that the areas under the curves are nearly preserved from the steady to the vibrating condition. Also note that the characteristic length changes but little if that length is taken from the half maximum pressure position on the pressure rise to the point of zero pressure. Adjustments of measured pressures to provide an estimate of pressure rise in the absence of vibration may now be undertaken. The adjusted maximum pressure may be found by dividing the area under the curve by one-half the characteristic length. Since the area tends to decrease with vibration and the length tends to increase, this is a conservative estimate. For example, in the case illustrated, the adjusted pressure is 94 percent of the N-wave peak pressure.

The foregoing discussion of vibration effects was considered to be independent of possible viscous effects. The boundary-layer, however, is a significant factor in the sensing of static-pressure changes across shock waves. The imposition of shock-wave pressure gradients on boundary layers of pressure-sensing instruments generally produces flow distortions which can be sensed both upstream and downstream of shock locations. This condition effectively results in tendencies for instrument-sensed pressure changes across shock waves to be less abrupt than pressure discontinuities across the shock waves in the absence of instruments. Such effects of boundary layer, as well as effects of vibration, in spreading and rounding off shock-wave pressure signatures are approximately accounted for by the described technique for adjusting wind-tunnel pressure measurements. The applicability of the adjustment technique may be uncertain, however, if the pressure-sensing arrangements are different from those employed in references 6 and 7 and in the present investigation.

REFERENCES

1. Walkden, F.: The Shock Pattern of a Wing-Body Combination, Far From the Flight Path. Aero. Quarterly, vol. IX, pt. 2, May 1958, pp. 164-194.

2. Randall, D. G.: Methods for Estimating Distributions and Intensities of Sonic Bangs. R. & M. No. 3113, British A.R.C., 1959.

3. Hubbard, Harvey H., Maglieri, Domenic J., Huckel, Vera, and Hilton, David A.: Ground Measurements of Sonic-Boom Pressures for the Altitude Range of 10,000 to 75,000 Feet. NASA TM X-633, 1962.

4. Morris, John: An Investigation of Lifting Effects on the Intensity of Sonic Booms. Jour. R.A.S., vol. 64, no. 598, Oct. 1960, pp. 610-616.

5. Carlson, Harry W.: An Investigation of Some Aspects of the Sonic Boom By Means of Wind-Tunnel Measurements of Pressures About Several Bodies at a Mach Number of 2.01. NASA TN D-161, 1959.

6. Carlson, Harry W.: An Investigation of the Influence of Lift on Sonic-Boom Intensity by Means of Wind-Tunnel Measurements of the Pressure Fields of Several Wing-Body Combinations at a Mach Number of 2.01. NASA TN D-881, 1961.

7. Carlson, Harry W.: Wind-Tunnel Measurements of the Sonic-Boom Characteristics of a Supersonic Bomber Model and a Correlation With Flight-Test Ground Measurements. NASA TN X-700, 1962.

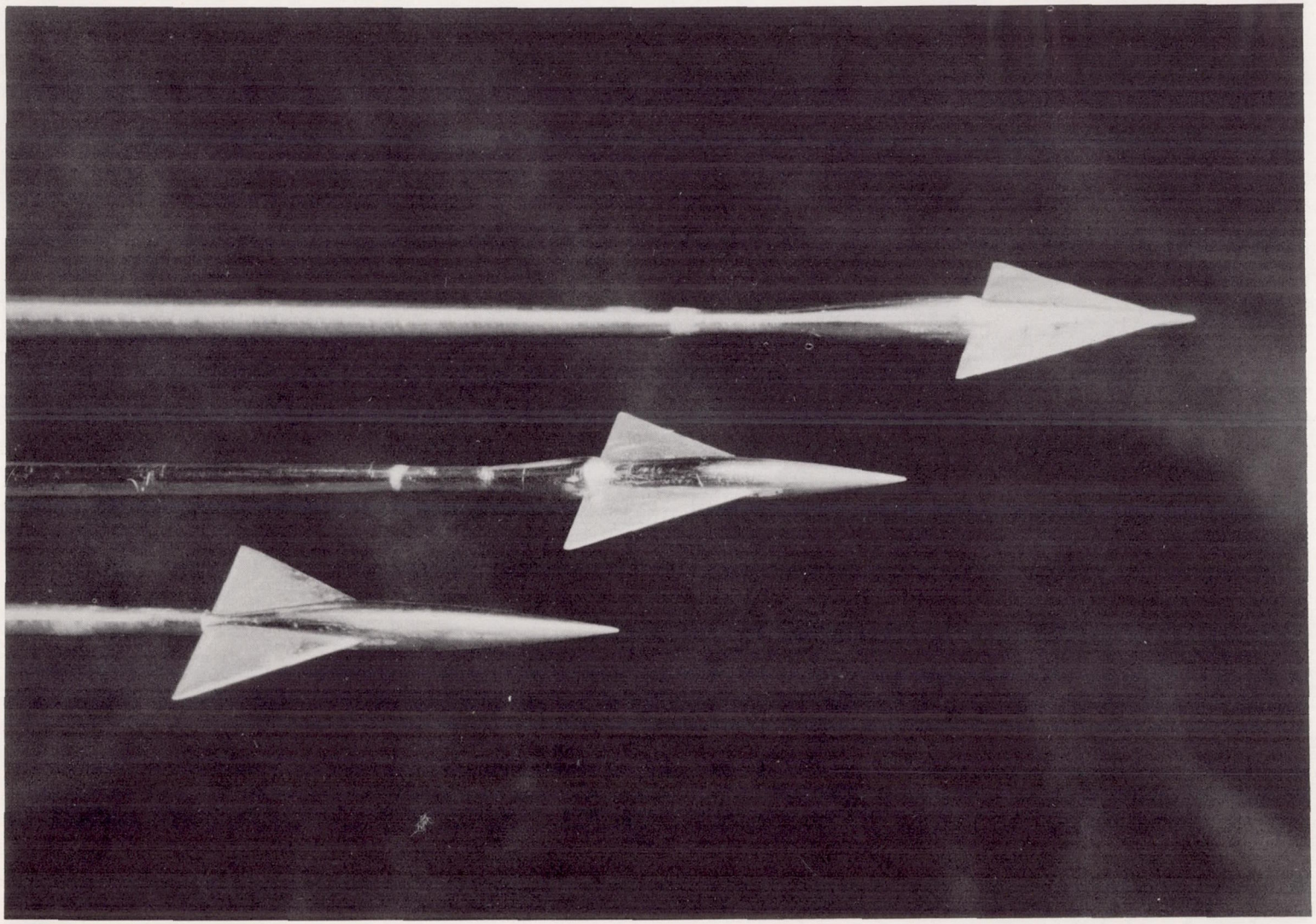

Figure 1.- Test models. L-62-2087

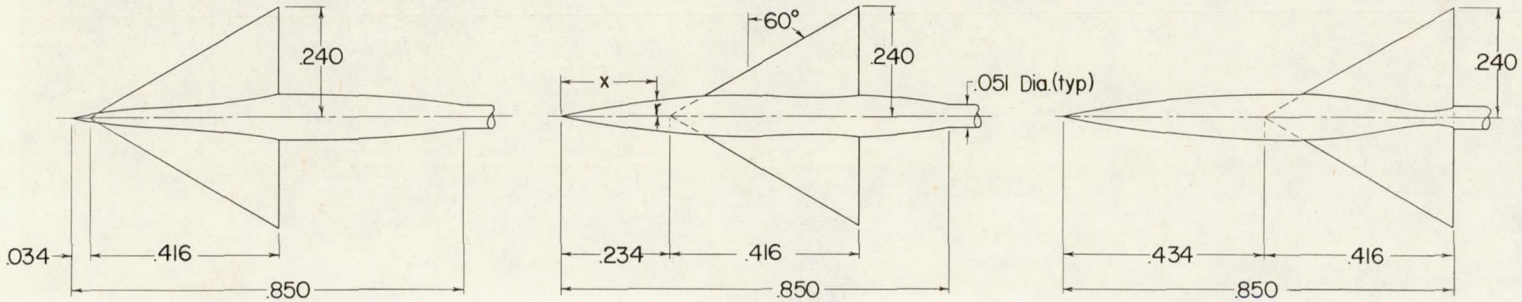

Model A

x	r
0	0
.050	.0095
.100	.0150
.150	.0200
.200	.0220
.250	.0260
.300	.0300
.350	.0350
.400	.0410
.450	.0495
.500	.0500
.550	.0495
.600	.0480
.650	.0455
.700	.0420
.750	.0375
.800	.0320
.850	.0255

Model B

x	r
0	0
.050	.0095
.100	.0180
.150	.0255
.200	.0320
.250	.0375
.300	.0420
.350	.0440
.400	.0450
.450	.0440
.500	.0420
.550	.0410
.600	.0410
.650	.0455
.700	.0420
.750	.0375
.800	.0320
.850	.0255

Model C

x	r
0	0
.050	.0095
.100	.0180
.150	.0255
.200	.0320
.250	.0375
.300	.0420
.350	.0455
.400	.0480
.450	.0495
.500	.0500
.550	.0490
.600	.0450
.650	.0380
.700	.0300
.750	.0200
.800	.0150
.850	.0255

Figure 2.- Details of models. All dimensions are in inches.

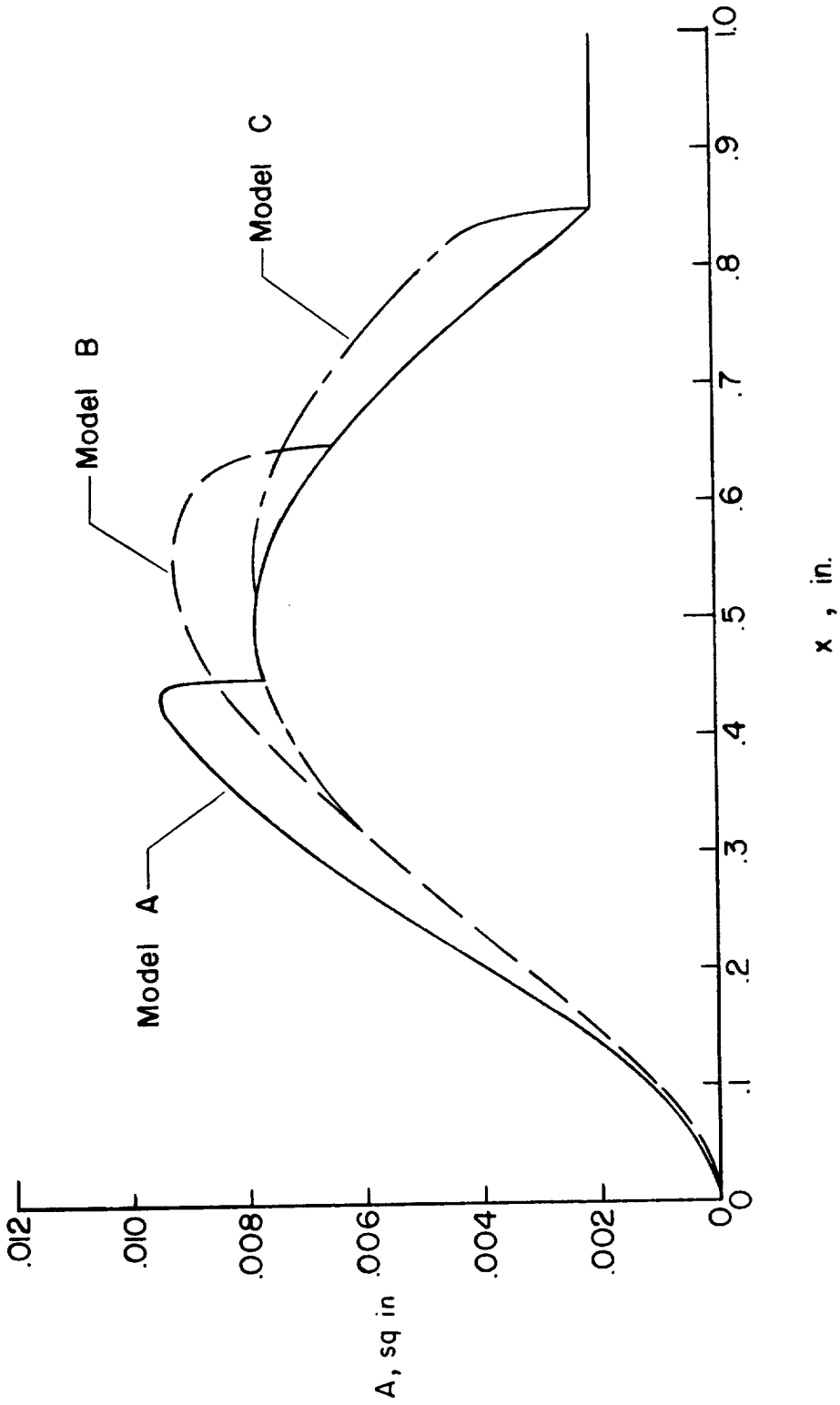

Figure 3.- Model cross-sectional-area distributions.

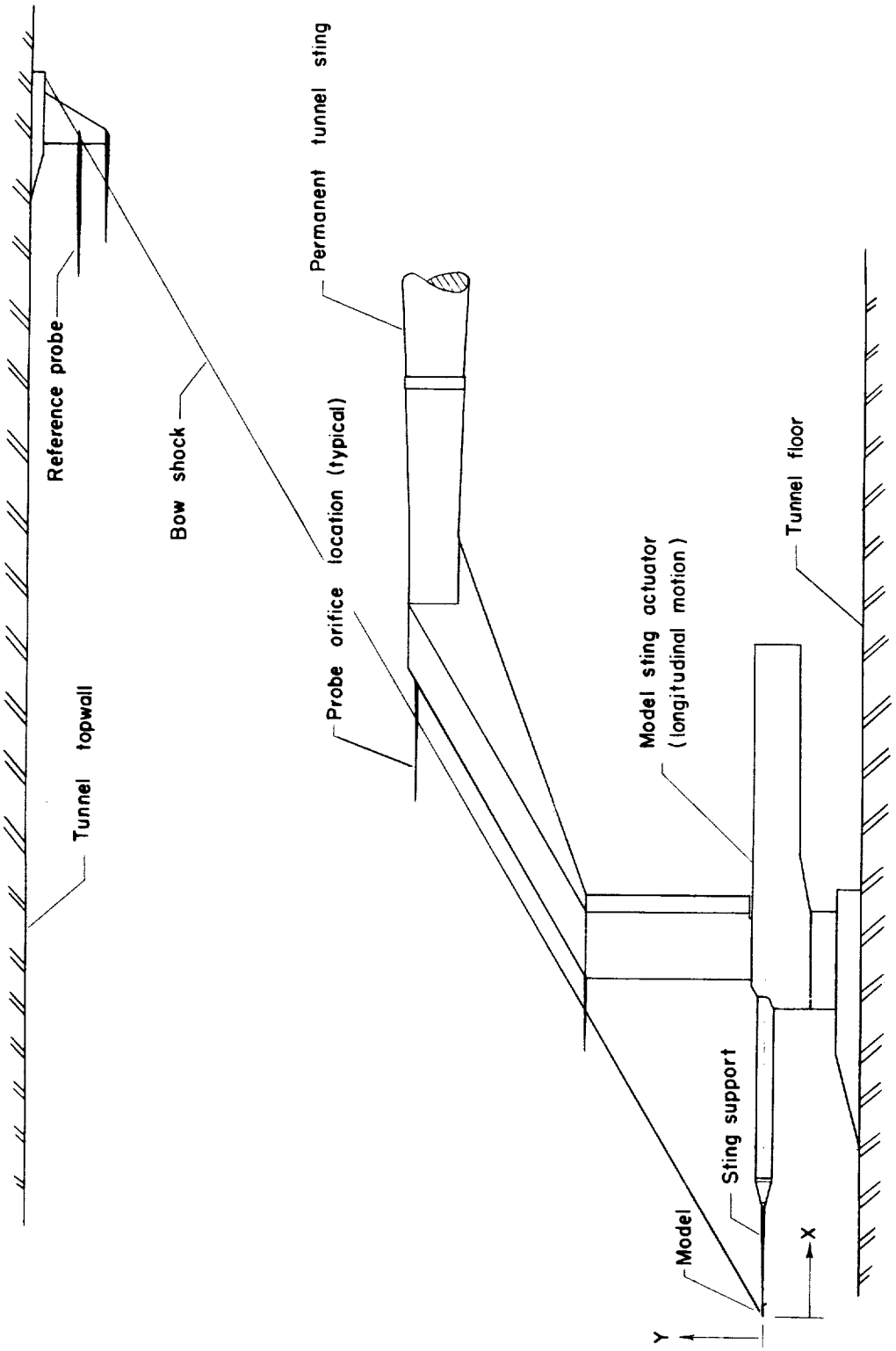

Figure 4.- Sketch of test setup. (Model is inverted.)

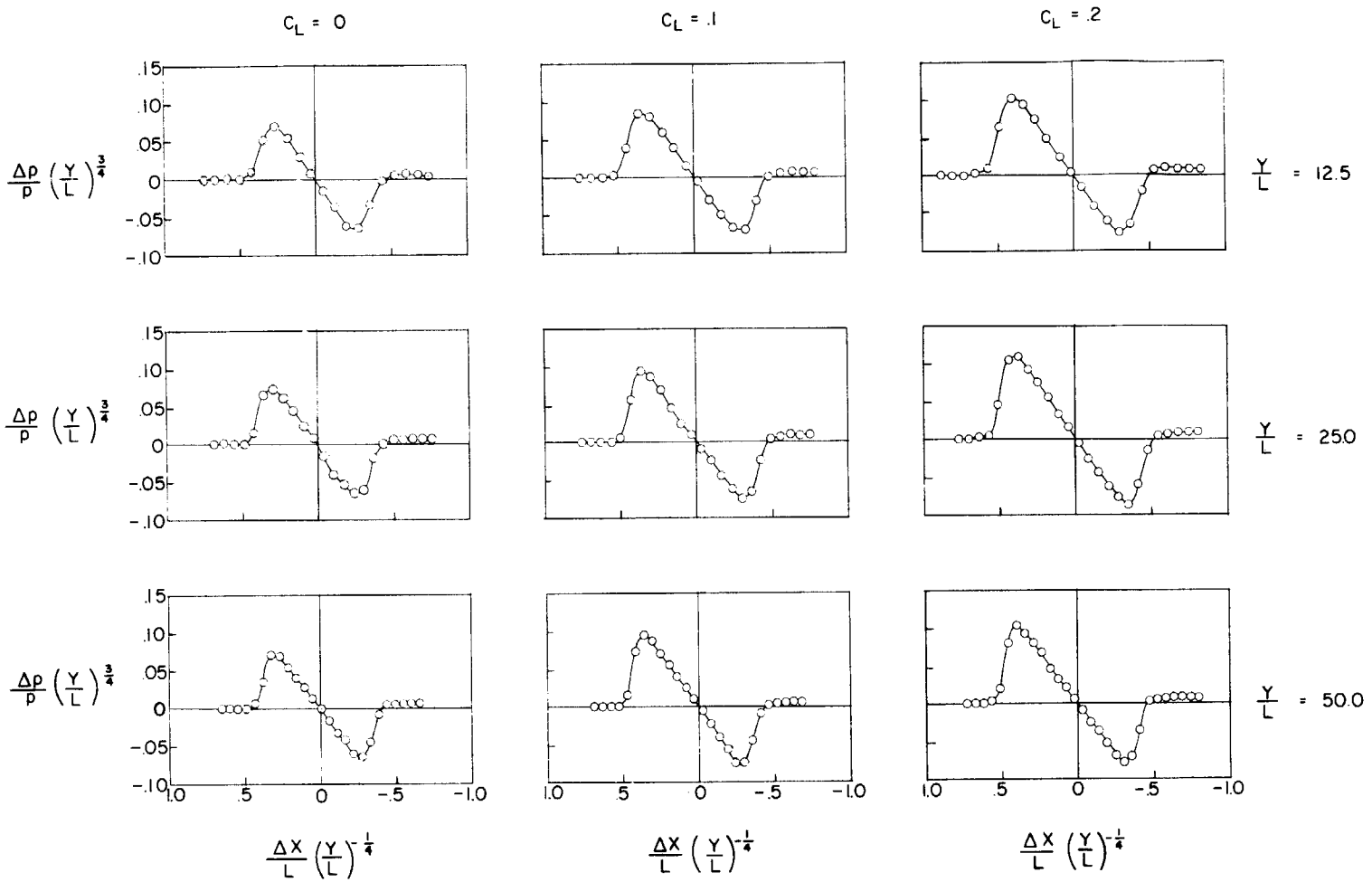

(a) Model A.

Figure 5.- Wind-tunnel measurements of the pressure signatures.

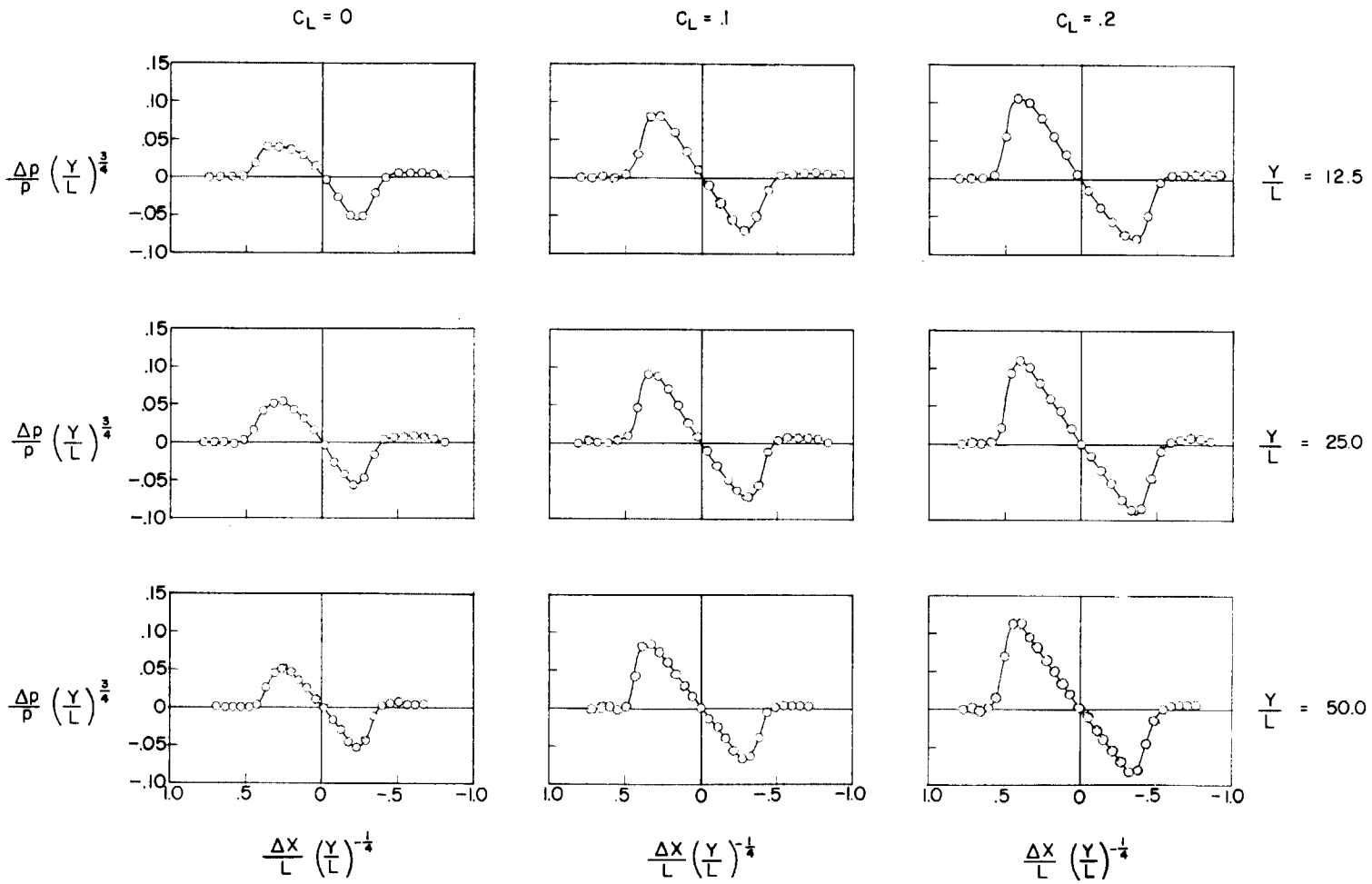

(b) Model B.

Figure 5.- Continued.

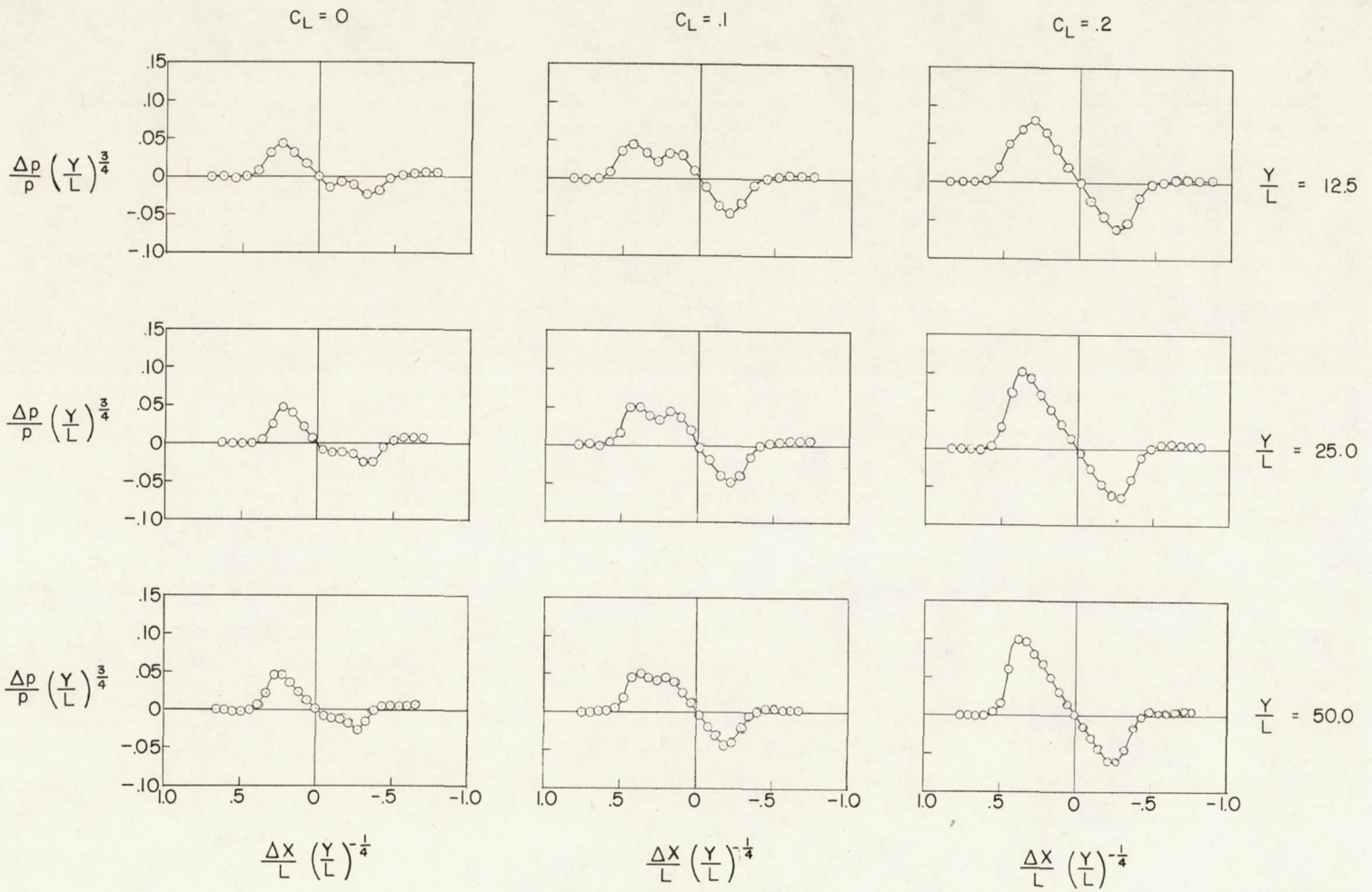

(c) Model C.

Figure 5.- Concluded.

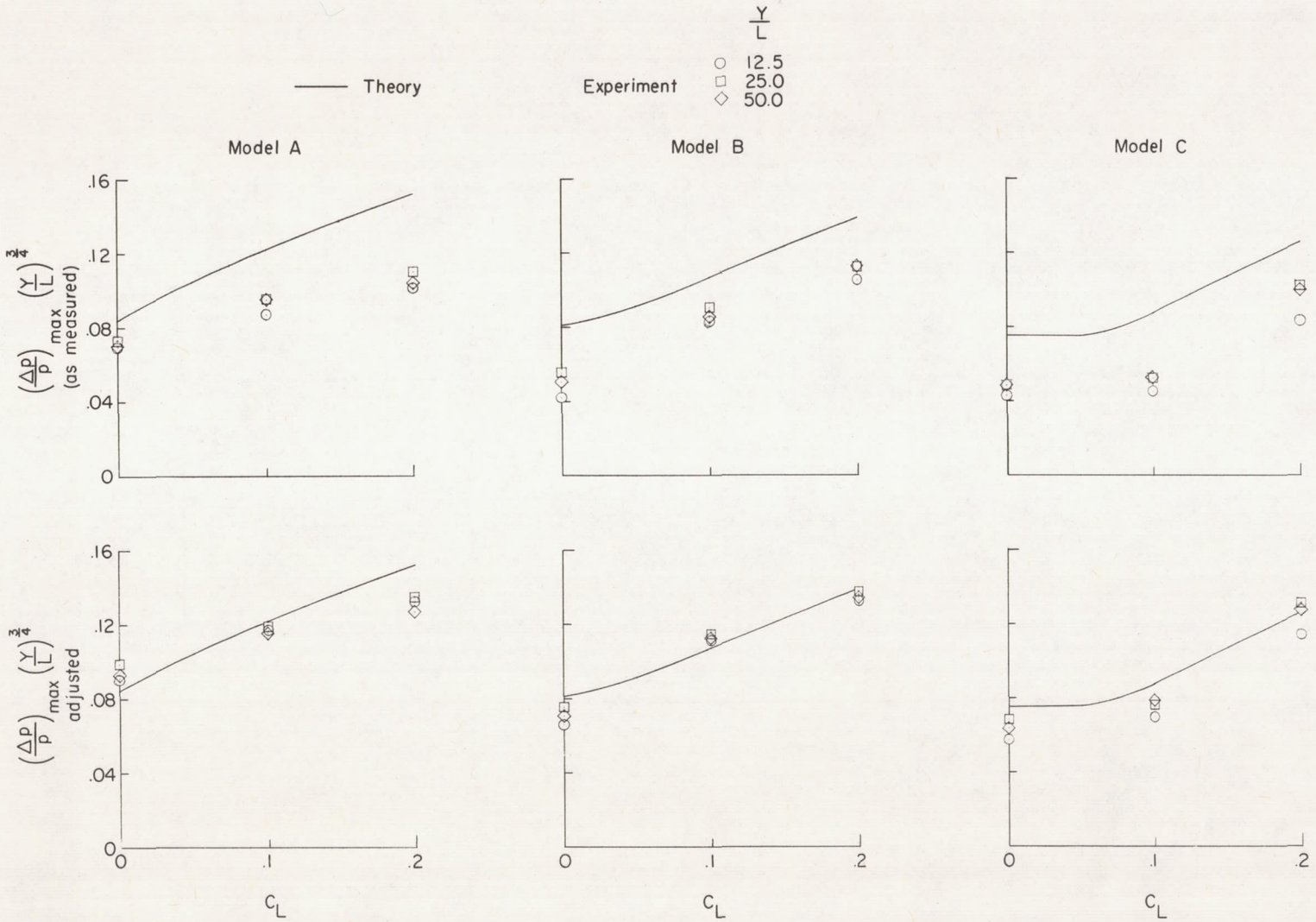

Figure 6.- Pressure rise of the bow shock from wind-tunnel measurements compared with theory.

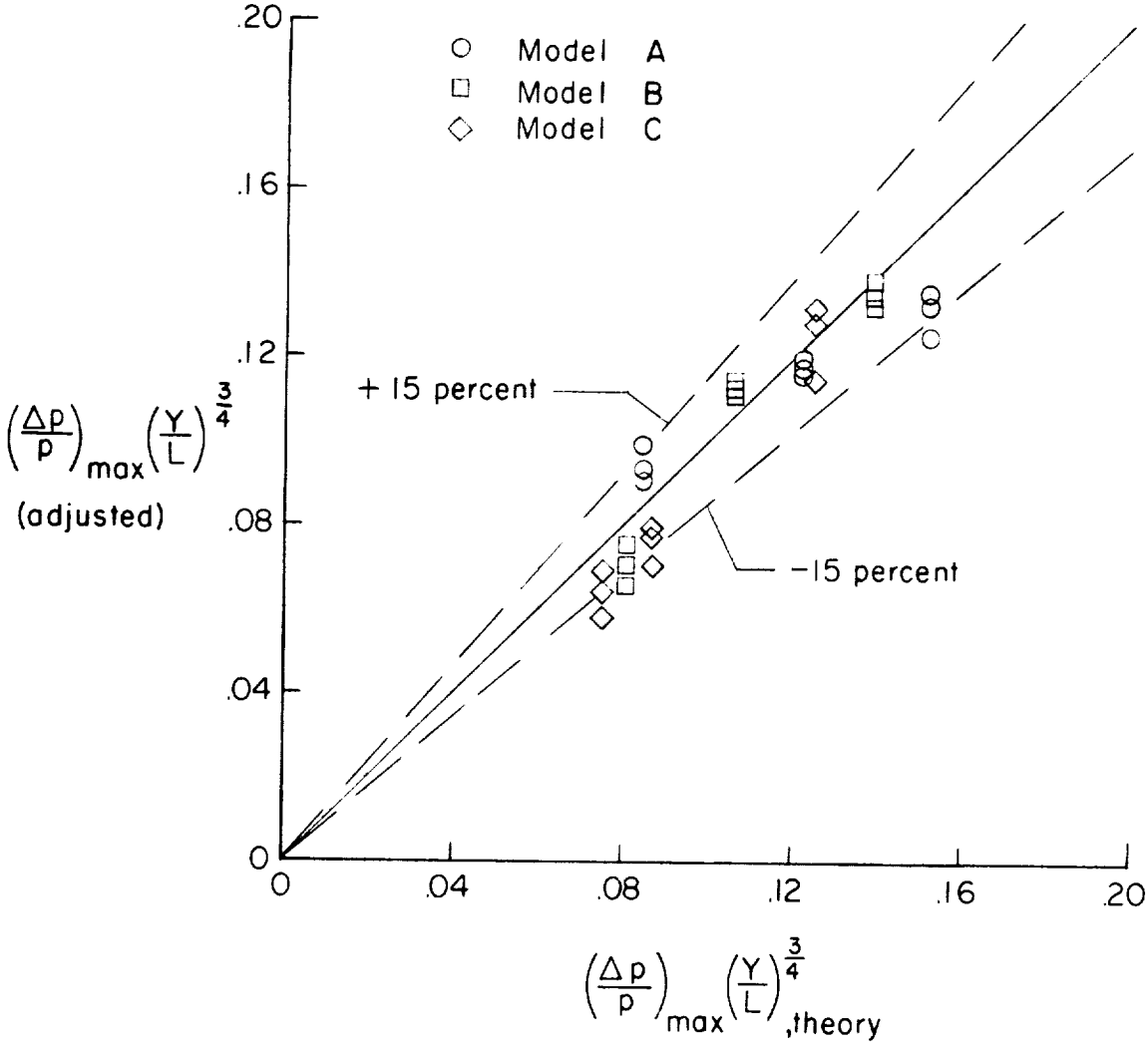

Figure 7.- Summary plot of the theoretical and measured pressures.